The American Journal of Pathology, Vol. 184, No. 8, August 2014

The American Journal of
PATHOLOGY
ajp.amjpathol.org

ANIMAL MODELS

Neonatal Thymectomy Favors *Helicobacter pylori*–Promoted Gastric Mucosa-Associated Lymphoid Tissue Lymphoma Lesions in BALB/c Mice

Delphine Chrisment,[*†] Pierre Dubus,[‡] Lucie Chambonnier,[*†] Anaïs Hocès de la Guardia,[*†] Elodie Sifré,[*†] Alban Giese,[‡] Myriam Capone,[§] Camille Khairallah,[§] Pierre Costet,[¶] Benoît Rousseau,[‖] Christophe Hubert,[**] Odile Burlen-Defranoux,[††] Christine Varon,[*†] Antonio Bandeira,[††] Francis Mégraud,[*†] and Philippe Lehours[*†]

From the Bacteriology Laboratory, EA 2406,[‡] National Center for Scientific Research (CNRS) UMR 5164 Innate Components of the Immune Response and Differentiation (CIRID),[§] the Animalerie Spécialisée,[¶] the Animalerie A2,[‖] the Functional Genomics Center,** the Genome Transcription Platform, University of Bordeaux, Bordeaux; INSERM U853,[†] Bordeaux; and the Lymphopoesis Unit,[††] INSERM U668, Institut Pasteur, Paris, France*

Accepted for publication
April 22, 2014.

Address correspondence to
Philippe Lehours, PharmD,
Ph.D., Bacteriology Laboratory,
Université de Bordeaux, and
INSERM U853, F-33076
Bordeaux, France.
E-mail: philippe.lehours@
u-bordeaux2.fr.

Neonatal thymectomy in BALB/c mice has been described as a model of gastric mucosa-associated lymphoid tissue (MALT) lymphoma (GML). By using this experimental system, we screened, for the first time to our knowledge, *Helicobacter pylori* GML-associated strains for their capacity to promote disease. A cohort of BALB/c mice underwent thymectomy at day 3 after birth (d3Tx). Successful thymic ablation was evaluated by the degree of lymphopenia in blood samples collected at 4 weeks of age. d3Tx and non-thymectomized controls were infected with either GML strains (B38 or B47) or control strains (SS1 or TN2GF4). Gastric samples collected at 6, 12, and 18 months after infection were studied for bacteria content, and submitted to histological, immunochemical, molecular, and immunological analyses. Severe gastric inflammation was only observed in d3Tx mice. In these animals, the gastric lamina propria was infiltrated with lymphoid cells organized in follicles composed of B cells with few infiltrating T cells. PCR of D/J IgH gene segments proved the monoclonality of infiltrating B cells, which strongly correlated with the presence of lymphoepithelial lesions. B-cell infiltrates were particularly prominent in mice infected with the B47-GML strain. No pathological changes were detected in noninfected d3Tx mice. We identified new *H. pylori* isolates adapted to the mouse stomach with high potential of GML development, which is only revealed in hosts rendered lymphopenic by neonatal thymic ablation. *(Am J Pathol 2014, 184: 2174–2184; http://dx.doi.org/10.1016/j.ajpath.2014.04.008)*

The mucosa-associated lymphoid tissue (MALT)-type lymphomas are the most frequent extranodal entities usually found in organs normally devoid of lymphoid tissue, such as the stomach.[1,2] The development of gastric MALT lymphoma (GML) in humans is directly related to infection by *Helicobacter pylori*, but it only appears in a few infected individuals.[2,3] Chronic antigenic stimulation exerted by *H. pylori* on the gastric mucosa causes the appearance of dense lymphoid infiltrates containing small centrocytic B cells expressing several surface markers (CD20, CD79a, BclII, and IgM) typical of the marginal zone B cells of normal MALT. They occupy the lamina propria and are organized in reactional lymphoid follicles, destroying and replacing the glandular structures. At this stage, lymphoepithelial lesions (LELs) may occur, characterized by the invasion of the epithelium of the gastric glands by proliferating B cells and epithelial cell destruction.[4] Many nonneoplastic T lymphocytes are associated with lymphoma cells with a predominance of $CD4^+$ T-helper cells.[5]

A better understanding of the pathophysiological characteristics of this lymphoma has been hampered by the difficulty in obtaining primary xenografts from surgical specimens of GML patients. Thus far, available animal

Supported by Société Nationale Française de Gastroentérologie grant, French Ministry of Research (A.H.d.l.G.), and Cancérople Grand Sud Ouest (A.G. and Experiment Histology Unit, University of Bordeaux).

D.C. and P.D. contributed equally to this work.

Disclosures: None declared.

http://dx.doi.org/10.1016/j.ajpath.2014.04.008

models used mainly rodents of the Murinae (mice) and Gerbillinae (mongolian gerbils) subfamilies, infected with three main *Helicobacter* species (namely, *Helicobacter felis*,[6–10] *Helicobacter heilmannii*,[9,11] and *H. pylori*[9,12–14]).

At 18 to 24 months after infection (PI), *H. felis*–infected BALB/c mice develop histological lesions evocative of GML (namely, multiple lymphoid infiltrates organized in follicles), composed of B cells with some infiltrating T cells (mainly $CD4^+$) associated with LELs.[6,9] However, lymphoid proliferation associated with these lesions regresses with antibiotic treatment.[7] These lesions re-emerge faster and more aggressively on reinfection, confirming the antigen-dependent nature behind lymphomagenesis.[7,10]

In BALB/c,[9,15] C57BL/6,[16] or mongolian gerbils,[11] *H. heilmannii* induces the development of GML to various degrees (25% to 66% of infected animals) and late after infection (18 to 24 months PI).[9,15]

For *H. pylori*, the *Helicobacter* species mainly involved in human GML, the situation is more complex. C57BL/6 mice appear to be a model for high-grade GML,[12] whereas BALB/c mice are described as a model for low-grade GML.[9,13,14] This dichotomy may reflect the immunogenetic predisposition of these two strains to generate types 1 and 2 helper T-cell responses, respectively. Only a small percentage (<20%) of infected BALB/c mice developed lymphomas 24 months PI, rendering this model difficult to use.[9,13,14] In addition, all previous studies have been based on an *H. pylori* strain (namely, the mouse stomach adapted strain called SS1)[17] because of its interesting property to infect mouse stomachs over a long time period. BALB/c mice that underwent thymectomy at day 3 after birth (d3Tx) have been described as an alternative model with a much earlier onset of gastric lymphomagenesis.[18–21] Thus, on infection at 6 weeks of age with the *H. pylori* TN2GF4 strain, a human Asian ulcer-associated strain,[22] most of these mice developed histological characteristics of GML at 12 months PI, whereas noninfected mice developed autoimmune gastritis.

To gain further insight into the mechanisms leading to GML, in this study, we identified new *H. pylori* GML-associated strains capable of colonizing the mouse stomach with high efficiency and endowed with a high potential to induce gastric lymphomagenesis in neonatally thymectomized BALB/c mice.

Materials and Methods

Mice and Thymectomy

Helicobacter-free BALB/cByJ mice were obtained from Charles River Laboratories (L'Arbresle, France). Mice were bred in our animal facilities under specific pathogen-free conditions. All experiments were performed in level 1 and level 2 animal facilities of the University of Bordeaux (Bordeaux, France) with the approval of institutional guidelines determined by the local ethical committee of the University of Bordeaux and in conformity with the French Ministry of Agriculture Guidelines on Animal Care and the French Committee of Genetic Engineering (approval number 50120143-A). Only female neonates were used for experiments. Neonatal thymectomy was performed on d3Tx. Briefly, the entire operation was performed on a heating carpet. Mice were anesthetized with isoflurane and ketamine/xylazine, then a thoracotomy was performed at the base of the neck. The thymus was quickly removed by suction with a micropipette. The opening was sewn closed with monofilament polyglyconate synthetic absorbable sutures, and the neonates were delivered to their mothers after being covered with urine. Successful thymectomy was monitored by the degree of lymphopenia at the age of 4 weeks (described later), and at sacrifice, mice with residual thymus were excluded. In case of doubt, the organ was removed and analyzed by a pathologist (P.D.).

H. pylori Strains and Infection Experiments

Among our collection of *H. pylori* GML-associated strains, two were used for their ability to colonize the stomachs of BALB/c mice (ie, strains B38 and B47).[23,24] Both are *cag* pathogenicity island (PAI) negative. The SS1[17] and TN2GF4 strains[21,22] were also tested in parallel. All *H. pylori* strains were cultured under microaerobic conditions (N_2, 85%; O_2, 5%; CO_2, 10%) at 37°C, as previously described.[25]

For mouse infection, *H. pylori* strains were grown on selective agar plates and collected in *Brucella* broth medium. Six-week-old mice were fasted to facilitate bacterial colonization and then force fed for 3 consecutive days with different strains at a dose of 10^8 *H. pylori* per mouse, as previously described.[26]

At the end of the experiment, part of the stomach of all infected mice was used for culture and then frozen at −80°C. Briefly, *H. pylori* culture was performed from the aseptically collected stomach, homogenized in PBS, seeded onto a selective medium, and incubated under microaerobic conditions at 37°C for 3 to 10 days, as previously described.[26]

Histological and Immunohistochemistry Experiments

d3Tx mice were sacrificed at 6 and 12 months PI, and non-thymectomized controls (NTx) at 6, 12, and 18 months PI. Half of the stomach was fixed in formaldehyde. Sections (3 μm thick) from paraffin-embedded tissues were processed for H&E staining. H&E-stained sections were coded and examined blindly by a pathologist (P.D.) for the presence of lymphoid infiltrates and LELs. These features were graded on a 0- to 3-point scale, according to the following criteria[9]: for lymphocytic infiltration: 0, no change; 1, single or few small aggregates of lymphocytes; 2, multiple multifocal large lymphoid aggregates or follicles; 3, extensive multifocal lymphocytic infiltration often extending through the depth of mucosa, resulting in distortion of the epithelial surface; for LELs: 0, no LELs; 1, early or single LELs; 2, multiple well-formed LELs; 3, multiple LELs, resulting in extensive destruction of the epithelium. Hyperplasia,

oxyntic gland atrophy, and mucinous and pseudo-intestinal metaplasia were scored using a scale of 1 to 4, as previously described.[26]

For immunohistochemistry (IHC), sections (3 μm thick) from paraffin-embedded tissue were rehydrated, washed, and heated to 100°C for 30 minutes and then brought to room temperature for 30 minutes for antigen retrieval using a buffer (pH 9). Endogenous peroxidases were inhibited with 3% hydrogen peroxide (Sigma, Saint-Quentin Fallavier, France) in water for 5 minutes, and blocking with 5% bovine serum albumin was performed. B lymphocytes were identified with a polyclonal goat anti−Pax-5 antibody (1:50, clone M-20; Tebu-bio, Le Perray-en-Yvelines, France), the rat monoclonal antibody anti-CD45R (1:100, clone RA3-6B2; Santa Cruz, CA), and T cells with a polyclonal goat anti-CD3 (1:50, clone C-20; Tebu-bio). After overnight incubation at 4°C, these primary antibodies were revealed using a streptavidin−biotin−horseradish peroxidase−diaminobenzidine system (Dako, Copenhagen, Denmark). CD79α$^+$ B cells were identified by polyclonal goat antibody anti-CD79α (1:50, clone V20; CliniSciences, Nanterre, France) incubated with avidin-biotin peroxidase complex (Vectastain ABC kit; Vector Laboratories, Inc., Burlingame, CA). A gastric cell-cell adhesion protein, E-cadherin, was detected by a polyclonal mouse antibody anti−E-cadherin (1:200, clone 36/E-cadherin; BD Biosciences, San Jose, CA), labeled polymer−horseradish peroxidase anti-mouse DAKO Envision Systems (Dako), and revealed by an additional 10-minute incubation with liquid diaminobenzidine Substrate-Chromogen System (Dako) at room temperature. All slides were counterstained with hematoxylin, dehydrated, and mounted with Eukitt mounting medium (Labonord; VWR International, Fontenay-sous-Bois, France).

Slides were scanned using a digital slide scanner (MIRAX SCAN; 3DHISTECH Ltd, Budapest, Hungary) equipped with a Zeiss objective (Plan-Apochromat 40×; numerical aperture, 0.95; Carl Zeiss Microscopy GmbH, Jena, Germany) and a high-resolution color camera (HV-F22; Hitachi Kokusai Electric America Ltd, Woodbury, NY). The images were read using the Pannoramic Viewer software version 1.15.3 (3DHISTECH Ltd). The maximum resolution obtained for a 40× objective was 0.11 μm per pixel.

Evaluation of Lymphopenia after Thymectomy

An intracardiac puncture was performed at 4 weeks of age, and blood was collected for subsequent flow cytometry analyses. Samples were placed in 20 μL of 0.5 mol/L EDTA and centrifuged for 10 minutes at 1240 × g. Pellets were placed at 4°C for 10 minutes and centrifuged for 5 minutes at 1240 × g. Leukocyte pellets were then suspended in 300 μL of PBS buffer. CD3−activated protein C (APC; PharMingen/BD Biosciences), CD4−phosphatidylethanolamine (PE), and CD8−fluorescein isothiocyanate (FITC; PharMingen/BD Biosciences) were then used and analyzed on a fluorescence-activated cell sorting (FACS) Canto flow cytometer (Becton Dickinson, Le Pont De Claix, France). For each marker, the expression levels were expressed as a percentage of positive cells from the total number of gastric cells. A group of 31 NTx mice served as the control group to determine normal values of the corresponding leukocyte populations.

Flow Cytometry Analysis of Stomach Samples

Stomachs were cut into small fragments that were then subjected to two cycles of 20-minute incubations with smooth

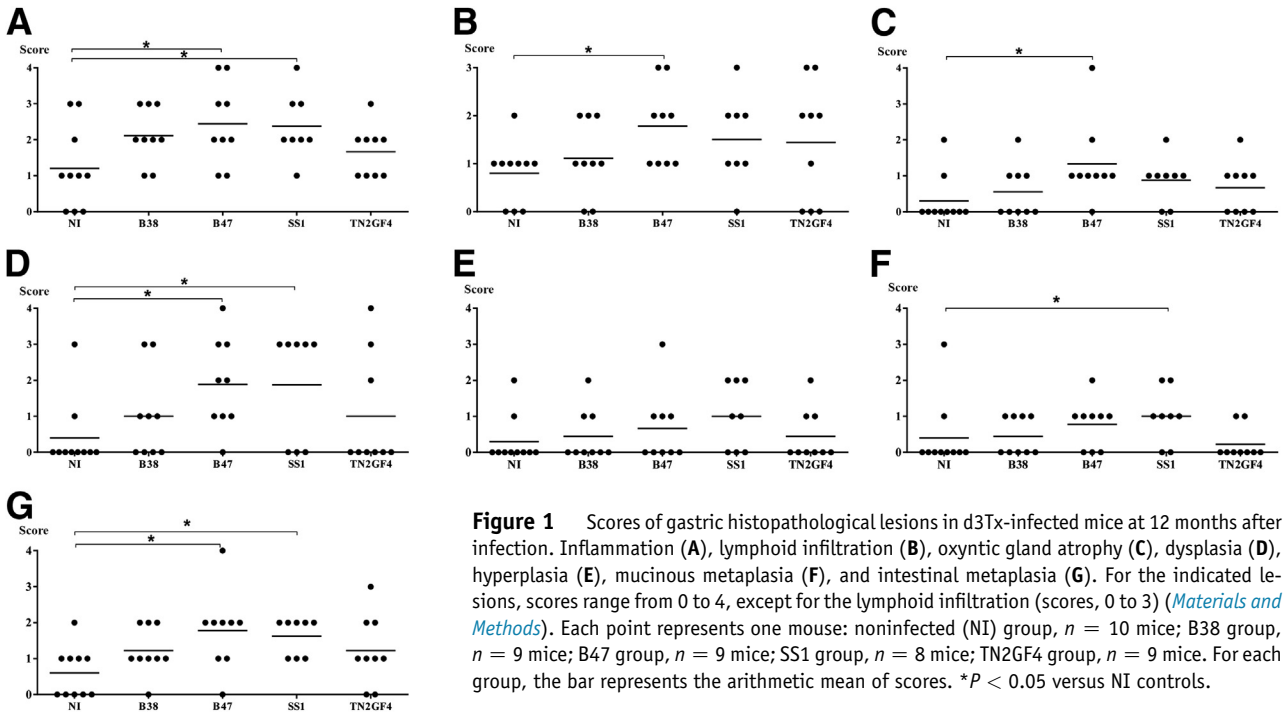

Figure 1 Scores of gastric histopathological lesions in d3Tx-infected mice at 12 months after infection. Inflammation (**A**), lymphoid infiltration (**B**), oxyntic gland atrophy (**C**), dysplasia (**D**), hyperplasia (**E**), mucinous metaplasia (**F**), and intestinal metaplasia (**G**). For the indicated lesions, scores range from 0 to 4, except for the lymphoid infiltration (scores, 0 to 3) (*Materials and Methods*). Each point represents one mouse: noninfected (NI) group, $n = 10$ mice; B38 group, $n = 9$ mice; B47 group, $n = 9$ mice; SS1 group, $n = 8$ mice; TN2GF4 group, $n = 9$ mice. For each group, the bar represents the arithmetic mean of scores. *$P < 0.05$ versus NI controls.

Table 1 Scoring for Lymphoid Infiltrates and Lymphoepithelial Lesions in d3Tx Mice, at 12 Months after Infection

	Lymphoid infiltrate scores				LEL scores			
Group of d3Tx mice	0	1	2	3	0	1	2	3
NI ($n = 10$)	3	6	1	0	9	1	0	0
B38 ($n = 9$)	2	4	3	0	5	3	1	0
B47 ($n = 9$)	0	4	3	2	3	5	1	0
SS1 ($n = 8$)	1	3	3	1	4	2	2	0
TN2GF4 ($n = 9$)	3	1	3	2	6	3	0	0
All infected mice ($n = 35$)	6	12	12	5	18	13	3	0

The scores are defined in *Materials and Methods*. For each group, the number of mice is indicated.

NI, noninfected.

shaking at 37°C in 10 mL HBSS ($Ca^{2+}Mg^{2+}$ free) (Gibco, Life Technologies, Saint Aubin, France) + 1 mmol/L HEPES (Gibco, Life Technologies) + 1 mmol/L dithioerythritol (Sigma-Aldrich) + 10% fetal bovine serum (FBS; Sigma-Aldrich). Debris were removed by passage through a 70 μm Falcon Cell Strainer (BD Biosciences). After filtration, the cells were centrifuged at 1870 × *g* for 5 minutes at 4°C, the supernatant was discarded, and the cells were washed twice in 10 mL of RPMI 1640 medium (GlutaMAX; Gibco, Life Technologies) + 8% FBS before staining. All cell suspensions were incubated with a viability marker, DAPI (Invitrogen, Cergy Pontoise, France) in a volume of 200 μL PBS + 2% FBS for 15 minutes at 4°C. All labeled antibodies were from PharMingen/BD Biosciences: T lymphocytes were characterized using CD45-APC (clone 30-F11), CD3e-FITC (clone 145-2C11), CD8a-PECy7 (clone 53-6.7), CD4-APC (clone RM4-5), and γδ T-cell receptor–PE (clone GL3). B lymphocytes were characterized using CD21/CD35-APC (clone 7G6), CD5-FITC (clone 53-7.3), IgM-PECy7 (clone R6-60.2), and B220-PE (clone RA3-6B2). Other inflammatory cells (polymorphonuclears, monocytes, and dendritic cells) were identified by CD45-APC, Gr1-FITC (clone RB6-8C5), CD11b-PeCy7 (clone M1/70), and CD11c-PE (clone HL3). Cells were washed once and analyzed on an FACS Canto II flow cytometer (BD Biosciences) using FACS Diva software version 8.0 (BD Biosciences).

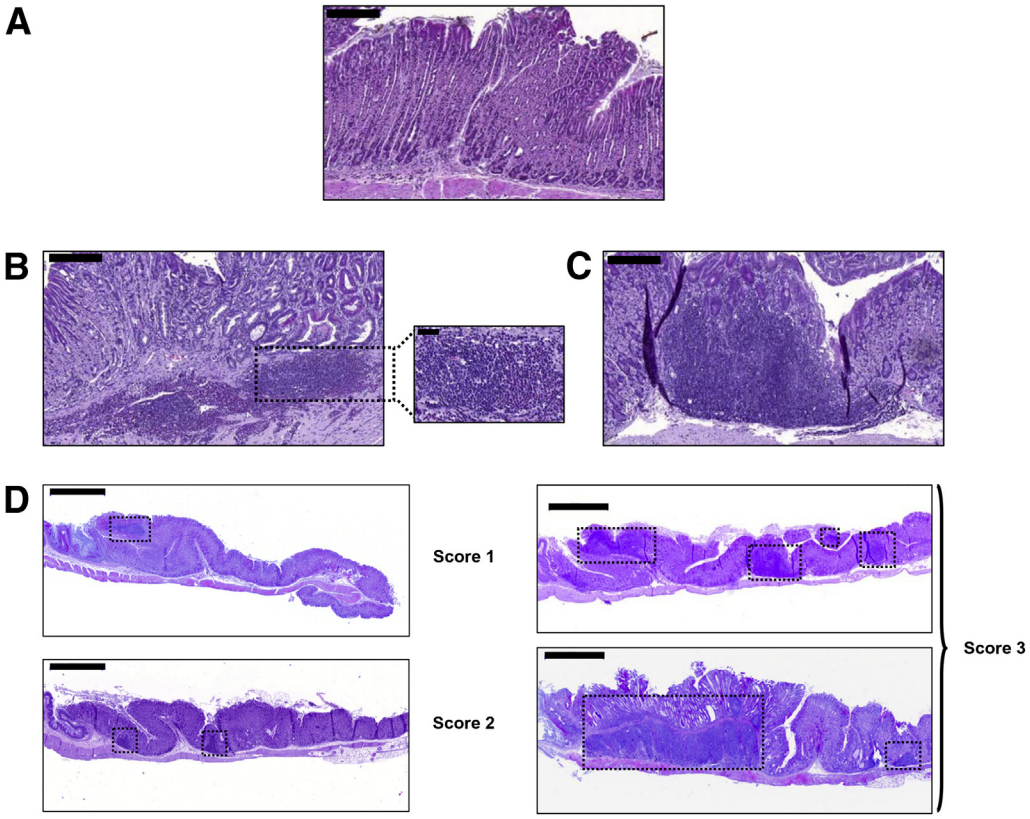

Figure 2 Histological and inflammatory aspects during *H. pylori* infection in thymectomized BALB/c mice at 12 months after infection. Sections (3 μm thick) from paraffin-embedded tissues were processed for H&E staining. **A:** Representative histopathological features of noninfected thymectomized (d3Tx) stomachs. The gastric mucosa has a normal aspect with no sign of inflammation or epithelial disorders. **B:** Representative inflammatory infiltrates, composed of lymphocytes and polymorphonuclears, found at the base of the mucosa of a B47-infected d3Tx mouse. A higher magnification of a polymorphonuclear infiltrate penetrating the muscularis mucosae is shown. **C:** In an SS1-infected mouse, there was a representative infiltrate of small lymphocytes with heterogeneous size invading epithelial structures. No lymphoepithelial lesions are visible in this case. **D:** Examples of lymphoid infiltrates. Score 1, single and small aggregate of lymphocytes in a B47-infected mouse; 2, multifocal large lymphoid aggregates or follicles in an SS1-infected mouse; 3, extensive multifocal lymphocytic infiltrations [B47-infected mouse (**top panel**)], often extending through the entire mucosa level, resulting in distortion of the epithelial surface [TN2GF4-infected mouse (**bottom panel**)]. **Dotted boxes** indicate the lymphoid infiltrates among the gastric mucosa. Scale bars: 200 μm (**A**–**C**); 50 μm (**B**, **inset**); 1000 μm (**D**).

DNA Extraction and PCR Amplification of the Immunoglobulin Heavy Chain

DNA extraction and immunoglobulin heavy chain amplification were performed for all d3Tx mice sacrificed at 12 months PI. Genomic DNA was extracted with the AllPrep DNA/RNA/miRNA Universal kit (Qiagen, Courtaboeuf, France) from the murine half stomach specimen stored at −80°C.

To detect immunoglobulin D-J_H rearrangement, PCR was performed in a reaction volume of 25 μL containing 5 μL of DNA extract, with a mixture of 1× PCR buffer (PlatinumTaq; Invitrogen), 1.5 mmol/L of $MgCl_2$ (Invitrogen), 1 μmol/L of each primer [DSF, 5′-AGGGATCCTTGTGAAGGGATC-TACTACTGTG-3′, JH4-FAM, and 5′-AAAGACCTGCA-GAGGCCATTCTTACC-3′ (Eurogentec, Seraing, Belgium), described by Kawamoto et al[27]] 125 μmol/L of dNTPs (Promega, Charbonnières, France), and 0.625 U of Platinum Taq polymerase (Invitrogen). DNA extract from mice with B-cell lymphoma was used as a positive control (a kind gift of Dr. Yves Denisot, University of Limoges, Limoges, France). Amplification was performed for 40 cycles. Amplified DNA products were loaded onto a 1% agarose gel containing 1 μg/mL de SYBR Safe DNA Gel Stain (Invitrogen) and were also analyzed by GeneScan fragment analysis on POP7

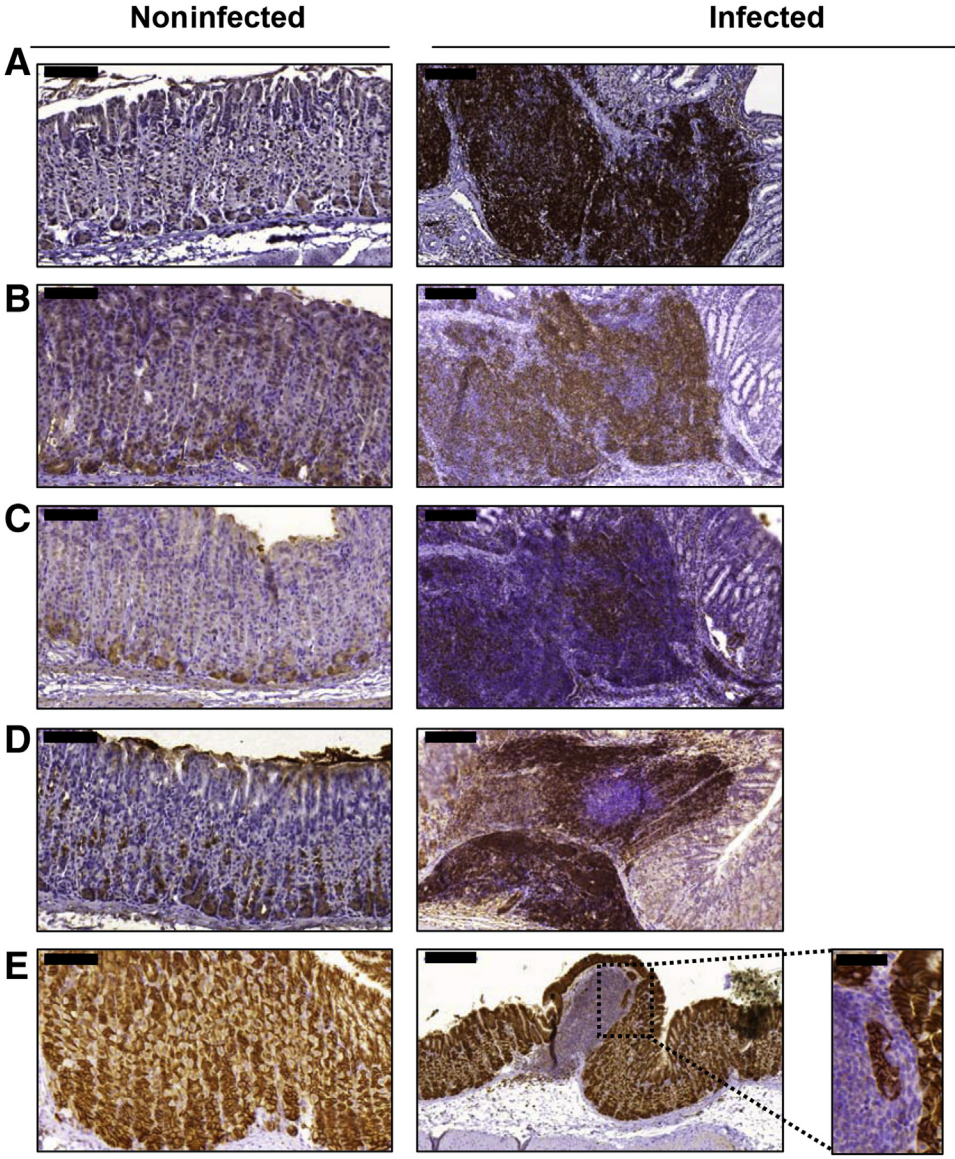

Figure 3 Analysis by IHC of the lymphoid infiltrates found in thymectomized BALB/c mice at 12 months after infection. **A**—**D:** Stomach sections of a B47-infected mouse and a noninfected control. Anti-CD45R (B220) (**A**), anti-Pax5 (**B**), anti-CD3 (**C**), and anti-CD79a (**D**) stainings show that infiltrating lymphocytes are mainly composed of B and T cells. Consecutive cuts of the same gastric biopsy specimen showing a lymphoid follicle with a B-cell region surrounded or including areas with exclusively T cells (**B** and **C**). B cells were predominantly $CD79a^+$, indicating a marginal zone phenotype. **E:** E-cadherin staining indicative of lymphoepithelial lesions. Example in an SS1-infected stomach of a lymphoid infiltrate clearly associated with an LEL. A higher magnification of this LEL is shown. For each marker, an example of a noninfected stomach is shown as a control. Scale bars: 100 μm (**A**—**E**, noninfected mice); 200 μm (**A**—**E**, infected mice); 50 μm (**E**, **inset**).

polymer (50-cm capillaries) with a 3130 XL Genetic Analyzer (Applied Biosystems) using GeneMapper software version 3.7 (Applied Biosystems).

A polyclonal profile was defined by the presence of several rearrangements on the CDR3 region of the IgH gene and represented by amplicons of different sizes and comparable intensity. An oligoclonal profile was defined by the restriction of the number of PCR fragments and a monoclonal profile by one single PCR amplicon with a fluorescence intensity 3× the highest background peak.

Statistical Analysis

Statistical analyses were performed using the nonparametric Mann-Whitney test. $P < 0.05$ was considered significant. All statistics were performed using GraphPad Prism version 6.0 (GraphPad Software, Inc., La Jolla, CA).

Results

Infected NTx Mice Do Not Develop Gastric Lesions

Noninfected NTx controls did not develop signs of gastric inflammation or any other pathological alterations with age (up to 18 months) (Supplemental Figure S1). NTx mice were infected at 6 weeks of age with B38, B47, or SS1 and TN2GF4 for control strains. All mice were colonized by *H. pylori*, as ascertained by culture and/or PCR performed at all experimental time points. At 6, 12, or 18 months PI, in a variable number of animals, a moderate leukocyte infiltration (median scores, <2) was observed in the upper part of the stomach, mainly composed of polymorphonuclears with no significant increase over time. Rare and small lymphoid infiltrates were sometimes found, but no LELs or epithelial lesions were apparent. These discrete signs of inflammation were also observed in the four infected groups.

Thus, we confirm the resistance of normal BALB/c mice to develop gastric lesions on *H. pylori* colonization and extend that resistance to two new strains.

Low Incidence of Autoimmune Gastritis in d3Tx Mice

Lymphopenia, a hallmark of adult neonatally thymectomized mice, was evaluated in the blood of d3Tx mice at the age of 4 weeks. Only animals with T-cell frequencies lower than the lowest outlier of NTx mice were considered (Supplemental Figure S2). In the selected pool of d3Tx mice, the frequency of T cells (or $CD4^+$ T cells) was on the average 20-fold lower than in age-matched NTx mice. These animals had no residual thymus at sacrifice, whereas a thymus was systematically observed in NTx animals, even at the age of 12 months.

At 6 months of age, noninfected d3Tx mice ($n = 10$) showed no signs of gastric inflammation or epithelial damage (Supplemental Figure S3). At 12 months, 30% (3/10) had inflammation scores ≥2. Small lymphoid infiltrates (scores 1 and 2) were found at the base of the mucosa in seven mice (Figure 1), but they were not associated with LELs with the exception of one mouse (Table 1). These histological aspects were compatible with a gastritis stage. Only one mouse showed significant oxyntic gland atrophy (score, 2) associated with hyperplasia (score, 2), mucinous metaplasia (score, 3), pseudo-intestinal metaplasia (score, 2), and dysplasia (score, 3) (Figure 1), a set of alterations compatible with established autoimmune gastritis.

Infected d3Tx Mice Develop Severe Lymphoma-Like Lesions

At 6 weeks of age, d3Tx mice were infected with B38, B47, or SS1 and TN2GF4 strains. At 6 months PI, many infected mice in all groups had moderate inflammatory infiltrates (median scores, <2) but no significant lymphoid infiltration or epithelial alterations (Supplemental Figure S3). At 12 months PI, most infected mice in all groups had significant mucosal inflammation (scores, 2 to 4) (Figure 1). Inflammatory infiltrates comprised polymorphonuclears present at the base of the mucosa with a tendency toward infiltration and destruction of the muscularis mucosae (Figure 2B) and/or lymphoid infiltrates

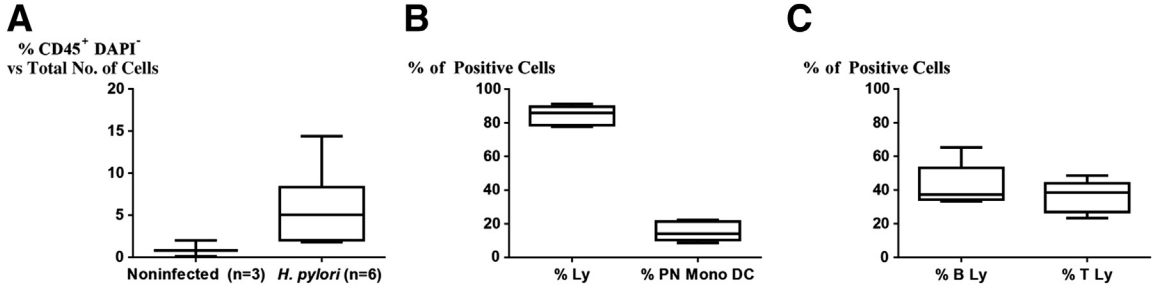

Figure 4 Inflammatory cells located in the gastric mucosa of nine d3Tx mice infected with *H. pylori* compared with three noninfected d3Tx mice, at 12 months after infection, as determined by flow cytometry. Two B47-infected, three SS1-infected, one TN2GF4-infected, and three noninfected mice were pooled in the analysis. **A:** Viable leukocytes ($CD45^+/DAPI^-$) in the gastric mucosa of the nine d3Tx mice were evaluated as the percentage of the total number of cells that were analyzed by the cytometer. **B:** Percentage of infiltrating lymphocytes ($CD3^+$ and $B220^+$ cells) and other inflammatory cells [polymorphonuclears, monocytes, and dendritic cells (PN Mono DC)] in the six infected d3Tx mice among $CD45^+$ cells. **C:** Percentages of infiltrating B lymphocytes (B Ly; $B220^+$) and T lymphocytes (T Ly; $CD3^+$). Data were obtained on an FACS Canto II flow cytometer using FACS Diva software. Data were expressed as a percentage of positive cells.

(Figure 2C), features that were absent in noninfected d3Tx mice (Figure 2A). Approximately 50% (17/35) of infected d3Tx mice had multiple lymphoid infiltrates, more or less extensive (scores, 2 to 4) (Figures 1 and 2D, Table 1), but only in the B47 group was the overall score of lymphoid infiltrates statistically different from that of noninfected d3Tx mice (Figure 1).

The presence of LELs was investigated by using H&E and E-cadherin IHC staining (Figure 3). Overall, LELs were found in 17/35 (48.5%) of infected mice (Table 1). Interestingly, these LELs were observed in most (14/17) mice with multiple and/or massive lymphoid infiltrates (scores, $\geq$2), whereas only one noninfected d3Tx mouse displayed similar lesions (Table 1). B47 infected mice showed the highest frequency of LELs (65%), compared with SS1 (50%), B38 (44%), and TN2GF4 (33%) infected groups.

Finally, significant epithelial damage was only apparent at 12 months PI and was most prominent in B47 infected mice, in particular with respect to oxyntic gland atrophy, dysplasia, and pseudo-intestinal metaplasia (Supplemental Figure S4).

In conclusion, d3Tx mice are highly susceptible to *H. pylori*–promoted lesions, reminiscent of those in gastric lymphomas in humans, with a higher incidence/severity for the B47 strain.

Oligoclonal/Monoclonal B Cells Predominate in the Lymphoid Infiltrates of Infected d3Tx Mice

For an in-depth characterization of the nature of the lymphoid infiltrates in infected d3Tx hosts, IHC staining was performed at 12 months PI. Infiltrating lymphocytes were mainly composed of B cells (Pax5$^+$ and CD45R$^+$) and T cells (Figure 3). A particular organization was observed for some of these lymphoid follicles with a visible region composed of B cells, which was surrounded or included areas composed exclusively of T cells when consecutive cuts of the same gastric biopsy specimen were compared (Figure 3). As also shown, B cells were predominantly CD79a$^+$.

To provide quantitative information on the relative frequency of lymphocyte subsets and to investigate surface markers that cannot be studied by IHC because of the lack of commercialized and/or validated antibodies for paraffin-embedded biopsy specimens from mice, flow cytometric analysis was performed on supernumerary d3Tx mice from the groups originally constituted, which were still alive after the final sacrifice time point (12 months PI). Flow cytometry results were considered for d3Tx-infected mice with significant lymphoid infiltrates (scores, >2) associated with LELs only because they were considered as representative of the leukocyte infiltration at a lymphoma stage. These studies addressed the B47, SS1, and TN2GF4 infected groups (two B47, three SS1, and one TN2GF4), and included three noninfected d3Tx mice as controls. As expected, 5× to 10× more lymphoid cells were recovered from infected than noninfected mice (Figure 4). For the six d3Tx mice included in the study, most lymphocytes were B cells (B220$^+$) (42.9% ± 12.3%), of which 78.9% ± 10.7% were CD5$^-$, CD21$^+$, and IgM$^+$, a phenotype typical of marginal zone B cells (Figure 5 and Supplemental Table S1). CD4$^+$ T cells predominated over CD8$^+$ T cells (CD4/CD8 ratio, 2.5 ± 1.0) (Figure 5 and Supplemental Table S1). In some infected mice, a small

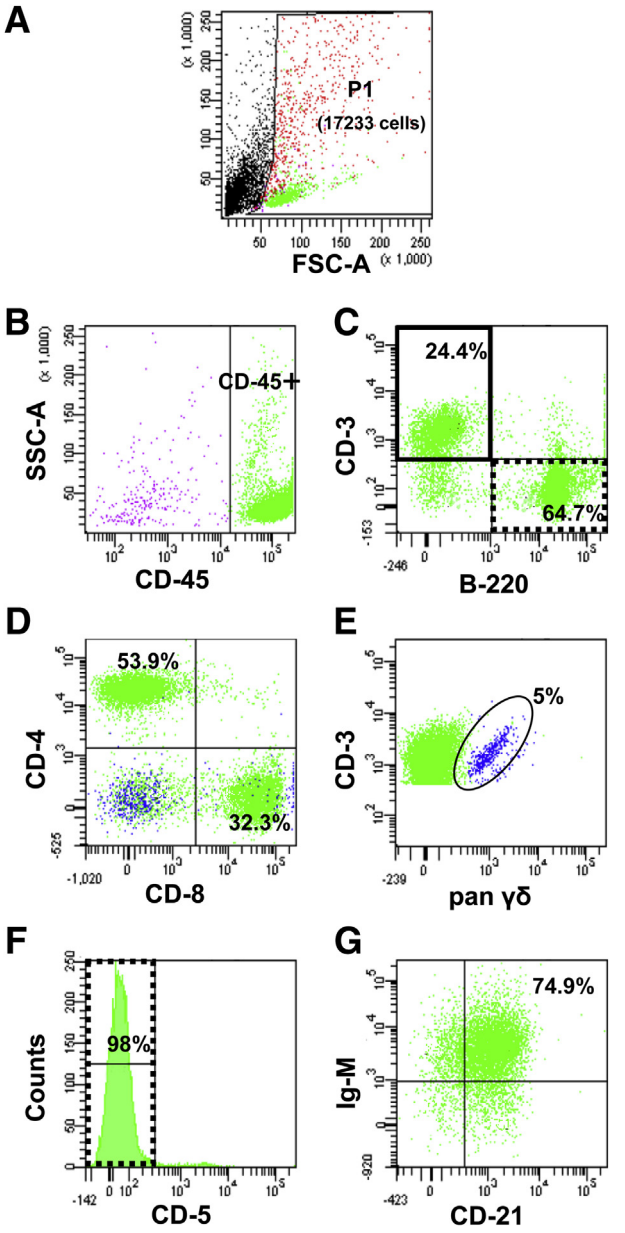

Figure 5 Characterization of the inflammatory cells located in the gastric mucosa of the d3Tx mice infected with *H. pylori* strain TN2GF4 at 12 months after infection, as determined by flow cytometry. **A:** Flow cytometry results obtained on the total number of gastric cells: P1 shows the cell population that was selected for analysis. Among P1, live cells were selected using a viability marker (DAPI-negative cells). **B:** Leukocytes were then selected by gating the CD45$^+$ population. **C:** The percentage of each subset within the CD45$^+$/DAPI$^-$ cell population is presented: T lymphocytes (CD3$^+$) and B lymphocytes (B220$^+$). The percentages of each subset among T lymphocytes are presented: T-helper lymphocytes (CD4$^+$) (**D**), T-cytotoxic lymphocytes (CD8) (**D**), and γδ T lymphocytes (**E**). Among B cells, the percentage of CD5$^-$ cells (**F**) and, for this subset, the percentage of double-positive IgM$^+$ CD21$^+$ cells (**G**). FSC-A, foward scatter-A; SSC-A, side scatter-A.

Table 2 Results of PCR Amplification of the CDR3 Region of the IgH Gene for d3Tx Mice at 12 Months after Infection and Correlation with the Presence of LELs

Group of d3Tx mice	CDR3 IgH PCR profiles			
	No amplification	Polyclonal	Oligoclonal	Monoclonal
NI ($n = 10$)	7 [0]	3 [1]	0 [0]	0 [0]
B38 ($n = 9$)	2 [0]	2 [0]	3 [2]	2 [2]
B47 ($n = 9$)	3 [0]	1 [1]	2 [2]	3 [3]
SS1 ($n = 8$)	0 [0]	1 [0]	4 [2]	3 [2]
TN2GF4 ($n = 9$)	5 [0]	0 [0]	2 [1]	2 [2]
All infected mice ($n = 35$)	10 [0]	4 [1]	11 [7]	10 [9]

For each group, the number of mice is indicated. The number of mice with LELs is indicated in brackets.
NI, noninfected.

compartment of γδ T cells (2.7% ± 2.0%) was found (Figure 5 and Supplemental Table S1). Other cell types (polymorphonuclears, monocytes, and dendritic cells) accounted for 15.2% ± 5.4% of the total lymphoid population (Figure 4 and Supplemental Table S1).

Finally, amplification of the CDR3 region of the IgH gene was used to study the level of clonality of infiltrating B cells in the stomachs of all d3Tx mice at 12 months PI (Table 2). No amplification was observed in 70% (7/10) of the noninfected mice and 28.6% (10/35) of the mice infected with *H. pylori*. A polyclonal profile was found in 11.4% (4/35) and 30% (3/10) in the infected and noninfected groups, respectively. More than 30% (11/35) of infected mice showed an oligoclonal profile, which was not observed in any of the 10 noninfected mice. Oligoclonality was observed in four of eight mice infected with SS1, three of nine mice infected with B38, two of nine mice infected with B47, and two of nine mice infected with TN2GF4. Interestingly, a single band was observed in 28.6% (10/35) of infected mice and in none of the noninfected mice (Table 2). Monoclonality was apparent in all infected groups: three of eight mice with SS1, two of nine mice with B38, three of nine mice with B47, and two of nine mice with TN2GF4. Most relevant, LELs were present in 76.2% (16/21) of mice with monoclonal or oligoclonal profiles.

In conclusion, in addition to the previously described pathological alterations, the identification of massive oligoclonal/monoclonal B-cell expansions with a marginal zone phenotype in *H. pylori*–infected d3Tx mice further indicates that this mouse model reproduces all lesions typical of low-grade gastric MALT lymphoma in humans.

Discussion

Neonatally thymectomized BALB/c mice provide a useful model to study the pathogenesis of *H. pylori*–promoted gastric MALT lymphoma. On infection with strains not associated with GML (eg, SSI and TN2GF4), these mice develop some typical histological lesions (namely, lymphoid infiltrates associated with LELs), considered as part of the pathognomonic signature of a lymphoma stage.[6,7,9]

By using this experimental model, the capacity of *H. pylori* strains obtained from patients with GML to promote lymphomagenesis was tested.

The first conclusion of our studies is that the resistance of normal BALB/c mice to develop *H. pylori*–promoted GML-like lesions appears independent of the strain's origin (GML associated or not) and of their capacity of adaption to the mouse stomach (single or multiple *in vivo* passages); rather, it relies on host factors that are somehow disrupted or weakened after neonatal thymic ablation (discussed later). This conclusion is based on the finding that, as described for the SSI and other non-GML *H. pylori* strains,[9,13,14] neonatal thymectomy is also a strict prerequisite for the emergence of lymphoma lesions induced by our GML-associated strains. This was most relevant for the B47 strain, which showed a surprising spontaneous ability of long-term colonization of the gastric mucosa (>1 year), without the need of undergoing multiple *in vivo* passages, a property also shared by the SS1 strain. Moreover, because our GML-associated strains are *cag* PAI negative and SS1 harbors an inactive *cag* PAI, we also conclude that this important virulence marker is not required for MALT pathogenesis, as already suggested.[24,28]

The second main observation is that all types of strains induced pathological alterations that in some hosts recapitulated the complete set of lesions and markers currently required for the diagnosis of low-grade gastric MALT lymphoma in humans.

Our in-depth histological analysis revealed that some B47 and SS1 infected d3Tx mice developed mucosal atrophy, metaplasia, and dysplasia, lesions that are frequently observed at the time of GML diagnosis in humans.[29,30] The presence of lymphoid infiltrates with a predominance of B cells with the phenotype expected for marginal zone B-cell lymphoma ($CD5^-$ $CD21^+$ IgM^+ $CD79a^+$)[5] was observed. As previously described, there was an emergence of lymphoid infiltrates associated with LELs, which constitutes a pathognomonic criterion. However, equally relevant in this respect was the high correlation between LELs and infiltrates composed of massive oligoclonal/monoclonal

B-cell expansions, which were detected in 60% of d3Tx-infected mice, a frequency similar to that found in humans.[31] Without this key element, it is virtually impossible to histologically distinguish lymphoid infiltrates from reactional lymphoid follicles, and a fortiori to conclude on the presence of true GML lesions. Few studies have included the analysis of the clonality of the B-cell infiltrates.[21,32] This might be explained by technical difficulties related to degradation of DNA on extraction from paraffin-embedded biopsy specimens, precluding the amplification of large PCR products. In our study, biopsy specimens were directly stored at −80°C until DNA extraction. In addition, we used methods allowing a better quantification of the abundance of the amplicons, which cannot be easily done after migration on an agarose gel.[27]

We also identified a set of indicators related to infiltrating T cells that are similar to those described in human GML. For example, there was a predominance of $CD4^+$ over $CD8^+$ T lymphocytes.[33,34] The predominance of the former subset is compatible with helper T-cell–dependent B-cell proliferation occurring early in low-grade GML, whereas the few CD8 T cells is consistent with the impaired cytotoxicity of tumor-infiltrating T cells described in humans,[34] both features contributing to lymphoma development. Interestingly, γδ T cells were detected at a low frequency in the lymphoid infiltrates. In normal individuals, these cells account for <5% of the T cells in the peripheral blood and secondary lymphoid organs, but are mainly distributed in the mucosal and epithelial tissues. By bridging innate and adaptive immunity, γδ T cells play important roles in the immune response against infection and tumors, but may also provide help for B cells, enhancing autoantibody production, as shown in autoimmune diseases.[35] Therefore, the presence of these cells in some infected animals may indicate a role in MALT pathogenesis, in particular in its autoimmune component.[36] Uchida et al[19] failed to detect γδ T infiltration in infected d3Tx mice. The great variability and low abundance of these cells among gastric samples may explain the discrepancy with our study.

We should point out that the incidence/severity of GML-like lesions varied among the groups of infected d3Tx mice, in agreement with Wang et al[13] in that *H. pylori* strain diversity may lead to different outcomes. This is illustrated by the more extensive and severe lesions induced by B47 compared with the B38 strain. It might be that B47 harbors particular GML-inducing antigens, a possibility that might be addressed with current genomic and proteomic tools. This is of interest in identifying in the future the specificity of infiltrating T cells that appear to recognize *H. pylori* antigens,[37,38] whereas this is not the case for the expanded oligoclonal/monoclonal B-cell populations.

Finally, a major difference with previous studies was the kinetics of appearance of GML-like lesions, which, in our experiments, were only apparent at 12 months PI versus 2 to 4 months PI.[18–21] We do not know the precise reasons for this delay, but they might be related to the low incidence of atrophic gastritis or overt inflammation in our noninfected d3Tx mice, which was high in the studies previously mentioned. Because d3Tx mice were selected on the basis of severe lymphopenia and the absence of residual thymus at sacrifice, the low incidence of autoimmune gastritis cannot be ascribed to incomplete thymectomy; however, it is likely to be related to the sanitary status of our mouse colony (ie, *Helicobacter hepaticus* free) and perhaps differences in diet. Incidentally, this observation suggests that the development of gastritis in neonatal thymectomized mice, although autoimmune in its nature, is favored by an environmental factor, a possibility that has not been previously considered. Collectively, our results and those of others strengthen the idea that the environmental and immunological contexts of the host before *H. pylori* infection are essential contributors to GML pathogenesis.

Why does neonatal thymectomy render hosts susceptible to GML lesions? Although regulatory T-cell–dependent systemic homeostasis is robust in mice thymectomized at birth, as indicated by the absence of the fatal scurfy/IPEX syndrome, they develop multiple organ-specific autoimmune diseases; these diseases are possibly due to holes in the repertoire of regulatory T cells whose T-cell receptor diversity is strongly reduced.[39] Future study of regulatory T cells could provide important information in understanding the emergence of GML in this model.[39] The investigation of the proinflammatory response could also provide interesting data concerning the $CD4^+$ T-cell cytokines that stimulate B-cell expansion in animals that underwent lymphomagenesis. This particular aspect is under study.

In conclusion, our study describes new *H. pylori* strains adapted to the mouse stomach and, in particular and for the first time, to our knowledge, GML-associated strains that exhibited interesting properties of lymphomagenesis. Compared with normal mice, neonatal thymectomy of BALB/c mice before infection with *H. pylori* generated favorable conditions for the development of immune lymphoid structures. Immunoallergic and autoimmune components could be the consequence of this surgery. Perspectives arising from the present study are diverse, in particular the understanding of inflammatory and molecular mechanisms.

Acknowledgments

We thank Prof. Victoria Korolik (Griffith University, Gold Coast, Australia) and Holly M.S. Algood (Vanderbilt University, Nashville, TN) for fruitful discussions, Dr. Antonio Bandeira (INSERM U668, Institut Pasteur, Paris, France) for introducing us to the expertise of neonatal mouse thymectomy, Anne Chopin for figure preparation, and Lindsay Megraud for the English revision of the manuscript.

A.H.d.l.G. performed all of the neonatal mouse thymectomy surgical procedures.

Supplemental Data

Supplemental material for this article can be found at *http://dx.doi.org/10.1016/j.ajpath.2014.04.008*.

References

1. Isaacson PG, Spencer J, Wright DH: Classifying primary gut lymphomas. Lancet 1988, 2:1148−1149
2. Ullrich A, Fischbach W, Blettner M: Incidence of gastric B-cell lymphomas: a population-based study in Germany. Ann Oncol 2002, 13: 1120−1127
3. Ben-Khelifa H: Gastric lymphoma: is the worldwide incidence rising? Gastrointest Endosc 2002, 56:955
4. Wotherspoon AC, Ortiz-Hidalgo C, Falzon MR, Isaacson PG: Helicobacter pylori-associated gastritis and primary B-cell gastric lymphoma. Lancet 1991, 338:1175−1176
5. Ferreri AJ, Ernberg I, Copie-Bergman C: Infectious agents and lymphoma development: molecular and clinical aspects. J Intern Med 2009, 265:421−438
6. Enno A, O'Rourke JL, Howlett CR, Jack A, Dixon MF, Lee A: MALToma-like lesions in the murine gastric mucosa after long-term infection with Helicobacter felis: a mouse model of Helicobacter pylori-induced gastric lymphoma. Am J Pathol 1995, 147:217−222
7. Enno A, O'Rourke J, Braye S, Howlett R, Lee A: Antigen-dependent progression of mucosa-associated lymphoid tissue (MALT)-type lymphoma in the stomach: effects of antimicrobial therapy on gastric MALT lymphoma in mice. Am J Pathol 1998, 152:1625−1632
8. Morgner A, Sutton P, O'Rourke JL, Enno A, Dixon MF, Lee A: Helicobacter-induced expression of Bcl-X(L) in B lymphocytes in the mouse model: a possible step in the development of gastric mucosa-associated lymphoid tissue (MALT) lymphoma. Int J Cancer 2001, 92:634−640
9. Mueller A, O'Rourke J, Grimm J, Guillemin K, Dixon MF, Lee A, Falkow S: Distinct gene expression profiles characterize the histopathological stages of disease in Helicobacter-induced mucosa-associated lymphoid tissue lymphoma. Proc Natl Acad Sci U S A 2003, 100:1292−1297
10. Mueller A, O'Rourke J, Chu P, Chu A, Dixon MF, Bouley DM, Lee A, Falkow S: The role of antigenic drive and tumor-infiltrating accessory cells in the pathogenesis of Helicobacter-induced mucosa-associated lymphoid tissue lymphoma. Am J Pathol 2005, 167:797−812
11. Flahou B, Haesebrouck F, Pasmans F, D'Herde K, Driessen A, Van Deun K, Smet A, Duchateau L, Chiers K, Ducatelle R: Helicobacter suis causes severe gastric pathology in mouse and mongolian gerbil models of human gastric disease. PLoS One 2010, 5:e14083
12. Wang X, Willen R, Andersson C, Wadstrom T: Development of high-grade lymphoma in Helicobacter pylori-infected C57BL/6 mice. APMIS 2000, 108:503−508
13. Wang X, Willen R, Svensson M, Ljungh A, Wadstrom T: Two-year follow-up of Helicobacter pylori infection in C57BL/6 and Balb/cA mice. APMIS 2003, 111:514−522
14. Thompson LJ, Danon SJ, Wilson JE, O'Rourke JL, Salama NR, Falkow S, Mitchell H, Lee A: Chronic Helicobacter pylori infection with Sydney strain 1 and a newly identified mouse-adapted strain (Sydney strain 2000) in C57BL/6 and BALB/c mice. Infect Immun 2004, 72:4668−4679
15. O'Rourke JL, Dixon MF, Jack A, Enno A, Lee A: Gastric B-cell mucosa-associated lymphoid tissue (MALT) lymphoma in an animal model of 'Helicobacter heilmannii' infection. J Pathol 2004, 203:896−903
16. Saito Y, Suzuki H, Tsugawa H, Imaeda H, Matsuzaki J, Hirata K, Hosoe N, Nakamura M, Mukai M, Saito H, Hibi T: Overexpression of miR-142-5p and miR-155 in gastric mucosa-associated lymphoid tissue (MALT) lymphoma resistant to Helicobacter pylori eradication. PLoS One 2012, 7:e47396
17. Lee A, O'Rourke J, De Ungria MC, Robertson B, Daskalopoulos G, Dixon MF: A standardized mouse model of Helicobacter pylori infection: introducing the Sydney strain. Gastroenterology 1997, 112:1386−1397
18. Oshima C, Okazaki K, Matsushima Y, Sawada M, Chiba T, Takahashi K, Hiai H, Katakai T, Kasakura S, Masuda T: Induction of follicular gastritis following postthymectomy autoimmune gastritis in Helicobacter pylori-infected BALB/c mice. Infect Immun 2000, 68: 100−106
19. Uchida K, Okazaki K, Debrecceni A, Nishi T, Iwano H, Inai M, Uose S, Nakase H, Ohana M, Oshima C, Matsushima Y, Kawanami C, Hiai H, Masuda T, Chiba T: Analysis of cytokines in the early development of gastric secondary lymphoid follicles in Helicobacter pylori-infected BALB/c mice with neonatal thymectomy. Infect Immun 2001, 69:6749−6754
20. Nishi T, Okazaki K, Kawasaki K, Fukui T, Tamaki H, Matsuura M, Asada M, Watanabe T, Uchida K, Watanabe N, Nakase H, Ohana M, Hiai H, Chiba T: Involvement of myeloid dendritic cells in the development of gastric secondary lymphoid follicles in Helicobacter pylori-infected neonatally thymectomized BALB/c mice. Infect Immun 2003, 71:2153−2162
21. Fukui T, Okazaki K, Tamaki H, Kawasaki K, Matsuura M, Asada M, Nishi T, Uchida K, Iwano M, Ohana M, Hiai H, Chiba T: Immunogenetic analysis of gastric MALT lymphoma-like lesions induced by Helicobacter pylori infection in neonatally thymectomized mice. Lab Invest 2004, 84:485−492
22. Watanabe T, Tada M, Nagai H, Sasaki S, Nakao M: Helicobacter pylori infection induces gastric cancer in mongolian gerbils. Gastroenterology 1998, 115:642−648
23. Thiberge JM, Boursaux-Eude C, Lehours P, Dillies MA, Creno S, Coppee JY, Rouy Z, Lajus A, Ma L, Burucoa C, Ruskone-Foumestraux A, Courillon-Mallet A, De Reuse H, Boneca IG, Lamarque D, Megraud F, Delchier JC, Medigue C, Bouchier C, Labigne A, Raymond J: From array-based hybridization of Helicobacter pylori isolates to the complete genome sequence of an isolate associated with MALT lymphoma. BMC Genomics 2010, 11:368
24. Lehours P, Menard A, Dupouy S, Bergey B, Richy F, Zerbib F, Ruskone-Fourmestraux A, Delchier JC, Megraud F: Evaluation of the association of nine Helicobacter pylori virulence factors with strains involved in low-grade gastric mucosa-associated lymphoid tissue lymphoma. Infect Immun 2004, 72:880−888
25. Ferreira-Chagas B, Lasne G, Dupouy S, Gallois A, Morgner A, Menard A, Megraud F, Lehours P: In vitro proinflammatory properties of Helicobacter pylori strains causing low-grade gastric MALT lymphoma. Helicobacter 2007, 12:616−617
26. Varon C, Dubus P, Mazurier F, Asencio C, Chambonnier L, Ferrand J, Giese A, Senant-Dugot N, Carlotti M, Megraud F: Helicobacter pylori infection recruits bone marrow-derived cells that participate in gastric preneoplasia in mice. Gastroenterology 2012, 142:281−291
27. Kawamoto H, Ikawa T, Ohmura K, Fujimoto S, Katsura Y: T cell progenitors emerge earlier than B cell progenitors in the murine fetal liver. Immunity 2000, 12:441−450
28. Taupin A, Occhialini A, RuskoneFourmestraux A, Delchier JC, Rambaud JC, Megraud F: Serum antibody responses to Helicobacter pylori and the cagA marker in patients with mucosa-associated lymphoid tissue lymphoma. Clin Diagn Lab Immunol 1999, 6:633−638
29. Herrera-Goepfert R, Arista-Nasr J, Alba-Campomanes A: Pathologic features of the gastric mucosa adjacent to primary MALT-lymphomas. J Clin Gastroenterol 1999, 29:266−269
30. Lamarque D, Levy M, Chaumette MT, Roudot-Thoraval F, Cavicchi M, Auroux J, Courillon-Mallet A, Haioun C, Delchier JC: Frequent and rapid progression of atrophy and intestinal metaplasia in gastric mucosa of patients with MALT lymphoma. Am J Gastroenterol 2006, 101: 1886−1893
31. Morgner A, Bayerdorffer E, Neubauer A, Stolte M: Gastric MALT lymphoma and its relationship to Helicobacter pylori infection: management and pathogenesis of the disease. Microsc Res Tech 2000, 48: 349−356

32. Craig VJ, Arnold I, Gerke C, Huynh MQ, Wundisch T, Neubauer A, Renner C, Falkow S, Muller A: Gastric MALT lymphoma B cells express polyreactive, somatically mutated immunoglobulins. Blood 2010, 115:581−591
33. Greiner A, Knorr C, Qin YF, Sebald W, Schimpl A, Banchereau J, MullerHermelink HK: Low-grade B cell lymphomas of mucosa-associated lymphoid tissue (MALT-type) require CD4O-mediated signaling and Th2-type cytokines for in vitro growth and differentiation. Am J Pathol 1997, 150:1583−1593
34. D'Elios MM, Amedei A, Manghetti M, Costa F, Baldari CT, Quazi AS, Telford JL, Romagnani S, Del Prete G: Impaired T-cell regulation of B-cell growth in Helicobacter pylori-related gastric low-grade MALT lymphoma. Gastroenterology 1999, 117:1105−1112
35. Su D, Shen M, Li X, Sun L: Roles of gammadelta T cells in the pathogenesis of autoimmune diseases. Clin Dev Immunol 2013, 2013:985753
36. Suarez F, Lortholary O, Hermine O, Lecuit M: Infection-associated lymphomas derived from marginal zone B cells: a model of antigen-driven lymphoproliferation. Blood 2006, 107:3034−3044
37. Hussell T, Isaacson PG, Crabtree JE, Spencer J: The response of cells from low-grade B-cell gastric lymphomas of mucosa-associated lymphoid tissue to Helicobacter pylori. Lancet 1993, 342:571−574
38. Hussell T, Isaacson PG, Crabtree JE, Spencer J: Helicobacter pylori-specific tumour-infiltrating T cells provide contact dependent help for the growth of malignant B cells in low-grade gastric lymphoma of mucosa-associated lymphoid tissue. J Pathol 1996, 178:122−127
39. Dujardin HC, Burlen-Defranoux O, Boucontet L, Vieira P, Cumano A, Bandeira A: Regulatory potential and control of Foxp3 expression in newborn CD4+ T cells. Proc Natl Acad Sci U S A 2004, 101: 14473−14478